Received 17 November 2019; revised 6 January 2020 and 7 February 2020; accepted 16 February 2020. Date of publication 21 February 2020; date of current version 27 February 2020. The review of this paper was arranged by Editor S. Reggiani.

Digital Object Identifier 10.1109/JEDS.2020.2975620

Normally-off p-GaN Gated AlGaN/GaN HEMTs Using Plasma Oxidation Technique in Access Region

XINKE LIU[1] (Member, IEEE), HSIEN-CHIN CHIU[2,3,4] (Senior Member, IEEE), CHIA-HAO LIU[2], HSUAN-LING KAO[2], CHAO-WEI CHIU[2], HSIANG-CHUN WANG[2], JIANWEI BEN[1], WEI HE[1], AND CHONG-RONG HUANG[2]

1 College of Materials Science and Engineering, College of Electronics and Information Engineering, Shenzhen University, Shenzhen 518060, China
2 Department of Electronic Engineering, Chang Gung University, Taoyuan 333, Taiwan
3 Department of Radiation Oncology, Chang Gung Memorial Hospital, Taoyuan 333, Taiwan
4 College of Engineering, Ming Chi University of Technology, Taipei 243, Taiwan

CORRESPONDING AUTHOR: H.-C. CHIU (e-mail: hcchiu@mail.cgu.edu.tw)

This work was supported by the Ministry of Science and Technology, Taiwan, under Grant MOST-108-2218-E182-006.

ABSTRACT Normally-off p-GaN gated AlGaN/GaN high electron mobility transistors (HEMTs) were developed. Oxygen plasma treatment converted a low-resistive p-GaN layer in the access region to a high-resistive GaN (HR-GaN); that oxygen plasma treatment used an AlN layer as an oxygen diffusion barrier layer to prevent further oxidizing of the underlying AlGaN barrier layer, and to ensure that the low-resistive p-GaN layer in the access region was fully oxidized. Relative to conventional p-GaN gated AlGaN/GaN HEMTs, these AlGaN/GaN HEMTs with HR-GaN layers achieved a lower drain leakage current of 4.4×10^{-7} mA/mm, a higher drain current on/off ratio of 3.9×10^{9}, a lower on-state resistance of 17.1 $\Omega\cdot$mm, and less current collapse.

INDEX TERMS p-GaN gate HEMT, normally-off, high-resistivity GaN.

I. INTRODUCTION

GaN-based high electron mobility transistors (HEMTs) a are emerging as promising candidates for next-generation power switching applications, due to their high mobility and large band gap. However, typical conventional AlGaN/GaN HEMTs are normally-on, featuring a negative threshold voltage, a high electron mobility, and a high-density two-dimensional electron gas (2DEG) [1]–[4]. However, normally-off devices operating at a positive threshold voltage are more desirable for power switching devices because of their simplified gate-drive topology and fail-safe operation [5]. Various approaches have been explored for making a normally-off device, such as F-based plasma treatment [6], [7], a p-GaN gate [8]–[12], and a recessed gate structure [13], [14]. Normally-off devices fabricated with p-GaN gate technology offer low on-state resistance and large positive threshold voltage, and such devices have drawn increasing attention for applications in power switching. However, to uniformly etch away the p-GaN in the non-gated access region and to overcome the plasma-induced damage during the p-GaN removal are extremely challenging tasks. Reactive Cl_2-based ion etching is typically used to remove the p-GaN layer. If such etching is not meticulously optimized, it may result in a rough surface due to plasma ionic bombardment and in surface defects or damage; these may cause gate lag [15]. To precisely control the etching depth, the chipmaker can insert an AlN etching stop layer between the p-GaN and barrier layers to achieve highly selective etching for better etching uniformity, lower gate leakage, and lower dynamic on-resistance [16]. However, the p-GaN in the access region becomes de-activated by hydrogen plasma treatment, which, instead of etching it away, converts low-resistivity p-GaN into high-resistivity GaN (HR-GaN) [17]. HR-GaN can help to realize AlGaN/GaN HEMTs with high breakdown voltage and low current collapse.

This work is licensed under a Creative Commons Attribution 4.0 License. For more information, see http://creativecommons.org/licenses/by/4.0/

The alloying process is challenging, in part because H–Mg bonds are easily broken at high temperatures; the long-term stability of deactivated p-GaN made by forming a H–Mg complex under high temperature (>200°C) warrants greater scholarly attention. Recently, oxygen plasma treatment has also been used to oxidize the p-GaN layer and form HR-GaN in the access region, but manufacturers do not yet have precise control over the depth of oxidation in the p-GaN layer [18]. In this study, an AlN layer, serving as an oxygen diffusion barrier layer, was introduced to prevent oxidation of the underlying AlGaN barrier layer in the access region during oxygen plasma treatment. High performance normally-off p-GaN gated AlGaN/GaN HEMTs were realized; in such HEMTs, the low-resistive p-GaN layers were fully oxidized and converted into HR-GaN.

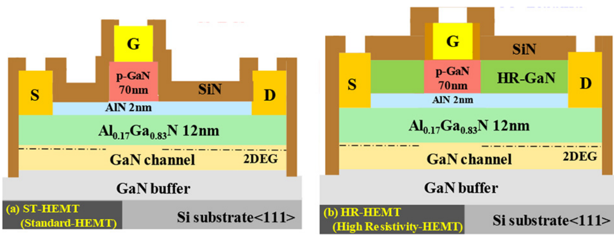

FIGURE 1. Device structure for (a) standard AlGaN/GaN HEMTs and (b) AlGaN/GaN HEMTs with HR-GaN layer after oxygen plasma treatment.

II. DEVICE STRUCTURE AND FABRICATION

The p-GaN/AlGaN/GaN HEMTs in this study were grown on 6-inch Si (111) substrates through metal organic chemical vapor deposition (MOCVD), shown in Fig. 1 (a) and (b). In each device, a 300-nm-thick undoped GaN channel was grown on top of a 4-µm-thick undoped GaN buffer transition layer. Subsequently, a 12-nm-thick $Al_{0.17}Ga_{0.83}N$ layer, 2-nm-thick AlN layer, and 70-nm-thick p-type GaN top layer were deposited. The Mg concentration was $3 \times 10^{19} cm^{-3}$; the device was thermally annealed within an MOCVD chamber at 720°C for 10 min in N_2 ambience, and the active Mg concentration was 1×10^{18} cm^{-3} according to the Hall measurement. For device fabrication, the mesa region was first formed with Cl_2-based reactive ion etching (RIE). High-density oxygen plasma treatment on the devices was produced by induced coupling plasma (ICP) for 20 min with an RF power of 300 W and a dc power of 100 W, during which the p-GaN layer was oxidized, converting the low-resistivity p-GaN into high-resistivity (HR) GaN, thus making the p/n junction invalid. Detailed X-ray photoelectron spectroscopy (XPS) results are analyzed in the next section. To fully oxidize the p-GaN in the access region, various O_2 treatment times were explored. To measure the oxidation depth, the oxidized p-GaN layer was etched by buffered oxide etch (BOE) and the oxidized depth was subsequently characterized by atomic force microscopy (AFM). Fig. 2 (a) presents oxidized depth as a function of O_2

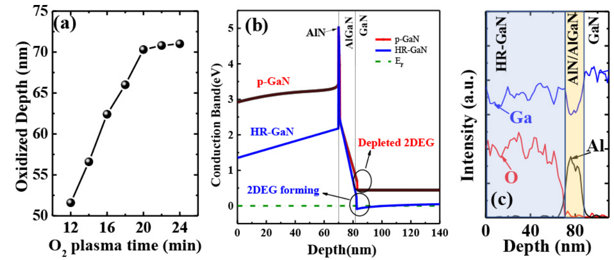

FIGURE 2. (a) oxidized depth as a function of O_2 plasma treatment; (b) Simulated band diagram of the access region with and without oxygen plasma treatment; (c) SIMS depth profiles of Ga, O, and Al of the access region with oxygen plasma treatment.

plasma treatment. After the selective removal of HR-GaN cap layer in source/drain region by RIE, Ti/Al/Ni/Au (25/120/25/150 nm) were deposited to form the source and drain metal electrodes, after which the device was annealed at 875°C for 35 s in N_2 ambience. Subsequently, Ti/Au (25/120 nm) were deposited as the gate electrode on top of p-GaN. Consequently, the conduction band in the channel was pulled down under the Fermi level, causing 2-dimensional electron gas (2DEG) to be formed in the channel, as illustrated in Fig. 2 (b). For a comparison, standard AlGaN/GaN HEMTs with RIE-etched p-GaN in the access region were also fabricated. Eventually, the Si_3N_4layers of two types of devices were passivated with plasma-enhanced chemical vapor deposition (PECVD). Both types of devices had a gate width of 100 µm, a gate length of 2 µm, a source-gate distance of 3 µm, and a gate–drain distance of 6 µm.

III. DEVICE RESULTS AND DISCUSSION

Fig. 2 (c) presents the SIMS profiles of Ga, Al, and O elements for p-GaN/AlN/AlGaN/GaN layers after 20 mins of oxygen plasma treatment. The signal of the elemental O that could be attributed to the oxygen plasma declined dramatically upon reaching the AlN/AlGaNepi layer, indicating that AlN is an effective diffusion barrier for O. The p-GaN layer was completely oxidized. During all oxygen plasma treatments, it can be assumed that the O concentration N_S at the surface of the p-GaN layer is always constant. The O concentration profile $N(x, t)$ within the p-GaN layer can be expressed using Fick's Law in one dimension:

$$N(x, t) = N_S erfc\left(\frac{x}{2\sqrt{Dt}}\right), \tag{1}$$

where x is the depth from the p-GaN surface, erfc is the complementary error function, t is the diffusion time, and D is O diffusivity in GaN. The function D depends on temperature (T):

$$D(T) = D_O \exp(-E_a/kT), \tag{2}$$

where D_O is the diffusivity (4.5×10^{-12} $cm^{-2}s^{-1}$) at infinite T, E_a is the activation energy (0.23 eV) [19]. As suggested by Equation (2), the characteristic O diffusion length in p-GaN is $2\sqrt{Dt}$, approximately equal to 87 nm (larger than

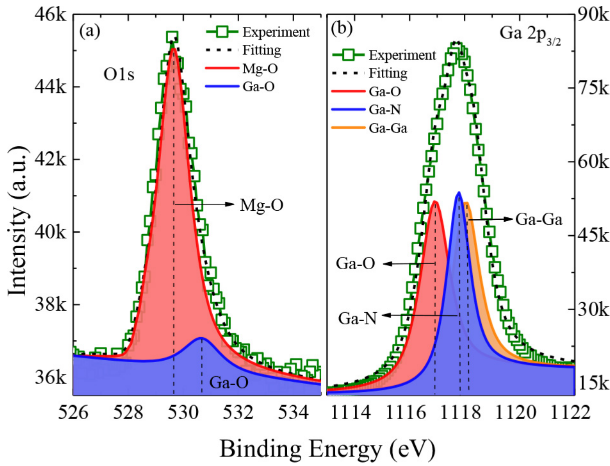

FIGURE 3. (a) XPS spectra of O1s and (b) XPS spectra of Ga $2p_{3/2}$ core-level of HR-GaN surface after O_2 plasma treatment.

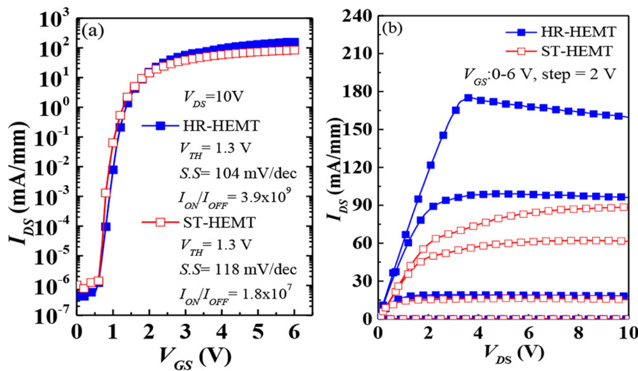

FIGURE 4. (a) Transfer characteristics (I_{DS}–V_{GS}) and (b) output characteristics (I_{DS}–V_{DS}) of AlGaN/GaN HEMTs with HR-GaN layer (HR-HEMTs) and standard AlGaN/GaN HEMTs (ST-HEMTs).

the thickness of p-GaN), if the temperature is assumed to be 473 K at the p-GaN surface. In the proposed device, the AlN layer serves as an oxygen diffusion barrier preventing further O diffusion into the underlying layers. Because the AlN layer protects the lower layers, a large process window of oxygen plasma treatment can be used for device fabrication. In addition, the material compositions of HR-GaN layers were analyzed by XPS, as shown in Fig. 3 (a) and (b). The green block is the experiment line, and the black dotted line is the fitting line. Fig. 3 (a) indicates that the O1s peaks comprise two components corresponding to Ga–O and Mg–O bonds; Fig. 3 (b) indicates that the Ga $2p_{2/3}$ peaks comprise three components corresponding to Ga–O, Ga–N, and Ga–Ga bonds. The XPS data indicate that the Mg–O and G–O signals for the oxidized p-GaN layer were clearly visible in the O1 peaks, which suggests that the p-GaN layer had been converted into a resistive layer, and no longer functioned as a p-type layer. Aside from the fact that Mg combined with O, the Ga–Ga signal was detected in the Ga $2p_{3/2}$ peaks; this demonstrates that the bonds had been interrupted [18].

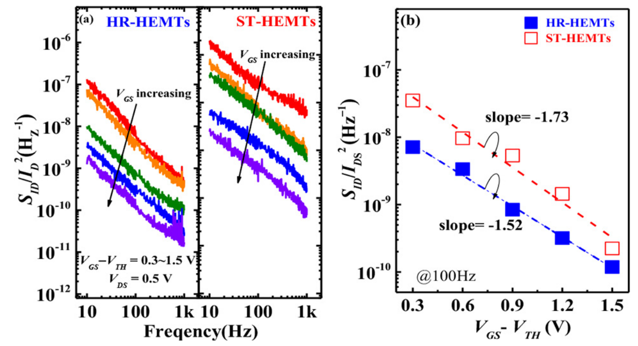

FIGURE 5. (a) LFN spectra characteristics for AlGaN/GaN HEMTs with and without HR-GaN layer; (b) S_{ID}/I_{DS}^2 as a function of gate voltage overdrive for AlGaN/GaN HEMTs with and without HR-GaN layer.

Fig. 4 (a) and (b) depict the transfer (I_{DS}–V_{GS}) and output (I_{DS}–V_{DS}) characteristics of AlGaN/GaN HEMTs with HR-GaN layer (HR-HEMTs) and standard AlGaN/GaN HEMTs (ST-HEMTs). As shown in Fig. 4 (a), the off-state drain current values for the HR-HEMT and ST-HEMT were 4.4×10^{-7} and 1.03×10^{-6} mA/mm, respectively, at $V_{GS} = 0$ V and $V_D = 10$ V. This result implies that O_2 plasma does not introduce extra plasma damage to the devices. By contrast, non-optimized conventional etching of p-GaN with corrosive Cl_2-based gases may result in many defects and dangling bonds [15]. These defects are traps; they block electrons' paths from the drain to source by hopping conduction.

In the present study, the threshold voltage (V_{TH}) value was 1.3 V in both types of devices. The drain ON/OFF current ratio (I_{ON}/I_{OFF}) values of the HR-HEMT and ST-HEMT devices were 3.9×10^9 and 1.8×10^7, respectively, and the subthreshold swing improved from 118 to 104 mV/decade in the HR-HEMT case. Fig. 4 (b) graphs the I_{DS}–V_{DS}output characteristic of the AlGaN/GaN HEMTs with and without HR-GaN. The maximum output current density I_{max} was 88 mA/mm at a gate bias of 6 V, and the on-resistance R_{on} was 31.8 Ω·mm for the ST-HEMTs. By contrast, I_{max} and R_{on} were 159 mA/mm and 17.1 Ω·mm, respectively, for the HR-GaN HEMTs. The higher output current performance of the HR-HEMTs may have been provided by the AlN stop layer that protected the AlGaN barrier layer. Compared with devices fabricated with a conventional etching process, HR-HEMTs have a favorable current density and low leakage current. The measured sheet resistances were 704 and 539 Ω per square for the control and the oxidized HR layer, respectively.

To analyze the trapping/de-trapping for HR-HEMTs and ST-HEMTs, low frequency noise (LFN) spectra were taken under five bias conditions from 10 to 1000 Hz. Fig. 5 (a) presents the drain current power spectral density S_{ID} normalized by the square of the drain current $I_{DS}{}^2$ versus the measurement frequency for both types of devices. Overall, the noise level of HR-HEMTs was lower than that for ST-HEMT by approximately one order of magnitude. The spectral fluctuation mechanism can be analyzed from

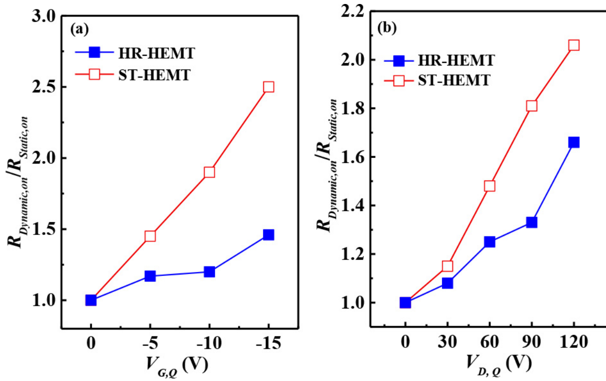

FIGURE 6. (a) Gate lag and (b) drain lag for AlGaN/GaN HEMTs with and without HR-GaN layer. The quiescent drain bias ($V_{D,Q}$) is 0 V during the gate lag measurement, and the quiescent gate bias ($V_{G,Q}$) is 0 V during the drain lag measurement.

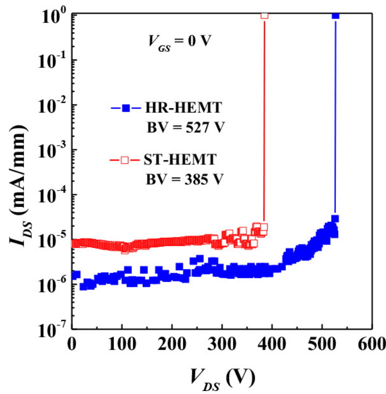

FIGURE 7. High-voltage breakdown characteristics of AlGaN/GaN HEMTs with and without HR-GaN layer.

the slope of S_{ID}/I_{DS}^2 versus gate overdrive V_G-V_{TH}. The mobility fluctuation model is dominant if the value of the slope is close to 1; the carrier number fluctuation model is dominant if the slope is close to 2 [18]. In this case, the values of the slope for S_{ID}/I_{DS}^2 versus V_G-V_{TH} plot shown in Fig. 5 (b) were −1.52 and −1.73 for HR-HEMTs and ST-HEMTs, respectively, indicating that for ST-HEMTs, carrier number fluctuation plays a more central role in noise.

Fig. 6 (a) and (b) graphs the dynamic on-state resistance over static on-state resistance ratio ($R_{Dynamic,on}$: $R_{Static,on}$) versus different quiescent gate or drain voltages. The pulse width and period time were 2 μs and 200 μs, respectively. The quiescent gate bias ($V_{G,Q}$) was swept from 0 V to −15 V with a step of −5 V and quiescent drain bias ($V_{D,Q}$) of 0 V. Obviously, the ST-HEMTs suffer from a larger current collapse due to the surface defects that result from the plasma etching process. Future studies should consider that the AlN layer may have a passivation effect for both types of devices. The drain lag measurement in Fig. 6 (b) exhibits the same trend. A component with an HR-GaN layer provided by oxygen plasma treatment can be integrated into AlGaN/GaN HEMTs; such devices will suffer less current collapse, owing to the AlN diffusion barrier design and low plasma damage. Overall, in the present study, the devices

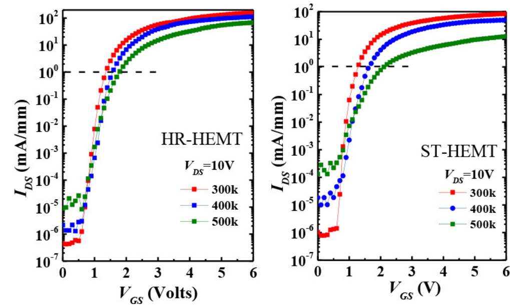

FIGURE 8. I_{DS}–V_{GS} characteristics at a drain voltage of 10 V of AlGaN/GaN HEMTs with and without HR-GaN layer under high temperature.

with AlN oxidation stop layers exhibited higher breakdown voltage and low current collapse. Fig. 7 presents the high voltage breakdown characteristics for both types of devices. In a device that had an HR-GaN layer provided by oxygen plasma treatment, the breakdown voltage V_{BR} increased from 360 to 545 V. Generally, the enhancement of V_{BR} is due to the reduction of peak electrical field near the gate edge at the drain side by the negative polarization charge at the interface of HR-GaN/AlGaN [21], [22]. When the temperature increased, the I_{DS}–V_{GS} curve of HR-HEMTs had a positive shift of approximately 0.47 V at a drain current of 1 mA/mm, which was smaller than the 0.87 V positive shift for ST-HEMTs. Furthermore, the current reduction at a gate voltage of 6 V for HR-HEMTs was less than that of ST-HEMTs. The thermal stability for the HR-HEMTs was superior because they experienced relatively minor surface damage.

IV. CONCLUSION

In this study, p-GaN gated AlGaN/GaN HEMTs with a HR-GaN layer have been fabricated using oxygen plasma treatment. Relative to standard p-GaN gated HEMTs, these HR-HEMTs had a lower drain leakage current of 4.4×10^{-7}mA/mm, a higher current on/off ratio of 3.9×10^9, and a higher output current of 159 mA/mm. Due to the minor process damage inflicted by oxygen plasma treatment, these HR-HEMTs had low on-state resistance (17.1 Ω·mm), high off-state breakdown voltage (530 V), and small current collapse. The technology of using oxygen plasma treatment to produce HR-GaN layers is a promising option for E-mode p-GaN gated AlGaN/GaN HEMTs in power electronics.

REFERENCES

[1] D.-B. Li *et al.*, "Direct observation of localized surface plasmon field enhancement by Kelvin probe force microscopy," *Light Sci. Appl.*, vol. 6, Aug. 2017, Art. no. e17038, doi: 10.1038/lsa.2017.38.

[2] X. Liu *et al.*, "Impact of *in situ* vacuum anneal and SiH_4 treatment on electrical characteristics of AlGaN/GaN metal-oxide-semiconductor high-electron mobility transistors," *Appl. Phys. Lett.*, vol. 99, Aug. 2011, Art. no. 093504, doi: 10.1063/1.3633104.

[3] X. Liu, Q. Liu, J. Wang, W. Yu, K. Xu, and J.-P. Ao, "1.2 kV GaN Schottky barrier diodes on free-standing GaN wafer using a CMOS-compatible contact material," *Jpn. J. Appl. Phys.*, vol. 56, Jan. 2017, Art. no. 026501, doi: 10.7567/JJAP.56.026501.

[4] O. Ambacher *et al.*, "Two dimensional electron gases induced by spontaneous and piezoelectric polarization in undoped and doped AlGaN/GaN heterostructures," *J. Appl. Phys.*, vol. 87, no. 1, pp. 334–344, Jan. 2000, doi: 10.1063/1.371866.

[5] M. A. Khan, Q. Chen, C. J. Sun, J. W. Yang, and M. Blasingame, "Enhancement and depletion mode GaN/AlGaN heterostructure field effect transistors," *Appl. Phys. Lett.*, vol. 68, no. 4, pp. 514–516, Jan. 1996, doi: 10.1063/1.116384.

[6] Y. Cai, Y. Zhou, K. J. Chen, and K. M. Lau, "High-performance enhancement-mode AlGaN/GaN HEMTs using fluoride-based plasma treatment," *IEEE Electron Device Lett.*, vol. 26, no. 7, pp. 435–437, Jul. 2005, doi: 10.1109/LED.2005.851122.

[7] Z. Tang *et al.*, "600-V normally off SiN_x /AlGaN/GaN MIS-HEMT with large gate swing and low current collapse," *IEEE Electron Device Lett.*, vol. 34, no. 11, pp. 1373–1375, Nov. 2013, doi: 10.1109/LED.2013.2279846.

[8] X. Hu, G. Simin, J. Yang, M. A. Khan, R. Gaska, and M. S. Shur, "Enhancement mode AlGaN/GaN HFET with selectively grown pn junction gate," *Electron. Lett.*, vol. 36, no. 8, pp. 753–754, Apr. 2000, doi: 10.1049/el:20000557.

[9] Y. Uemoto *et al.*, "Gate injection transistor (GIT)—A normally-off AlGaN/GaN power transistor using conductivity modulation," *IEEE Trans. Electron Devices*, vol. 54, no. 12, pp. 3393–3399, Dec. 2007, doi: 10.1109/TED.2007.908601.

[10] O. Hilt, A. Knauer, F. Brunner, E. Bahat-Treidel, and J. Würfl, "Normally-off AlGaN/GaN HFET with p-type Ga gate and AlGaN buffer," in *Proc. 24th Int. Symp. Power Semicond. Devices ICs*, Jun. 2010, pp. 347–350.

[11] T.-L. Wu *et al.*, "Forward bias gate breakdown mechanism in enhancement-mode p-GaN gate AlGaN/GaN high-electron mobility transistors," *IEEE Electron Device Lett.*, vol. 36, no. 10, pp. 1001–1003, Oct. 2015, doi: 10.1109/LED.2015.2465137.

[12] I. Hwang *et al.*, "1.6kV, 2.9 mΩ cm^2 normally-off p-GaN HEMT device," in *Proc. 24th Int. Symp. Power Semicond. Devices ICs*, Jun. 2012, pp. 41–44, doi: 10.1109/ISPSD.2012.6229018.

[13] W. Saito, Y. Takada, M. Kuraguchi, K. Tsuda, and I. Omura, "Recessed-gate structure approach toward normally off high-voltage AlGaN/GaN HEMT for power electronics applications," *IEEE Trans. Electron Devices*, vol. 53, no. 2, pp. 356–362, Feb. 2006, doi: 10.1109/TED.2005.862708.

[14] W. Li *et al.*, "Design and simulation of a novel E-mode GaN MIS-HEMT based on a cascode connection for suppression of electric field under gate and improvement of reliability," *J. Semicond.*, vol. 38, no. 7, Jan. 2017, Art. no. 074001, doi: 10.1088/1674-4926/38/7/074001.

[15] A. Tajalli *et al.*, "Impact of sidewall etching on the dynamic performance of GaN-on-Si E-mode transistors," *Microelectron. Rel.*, vol. 38, no. 7, pp. 572–576, 2018, doi: 10.1016/j.microrel.2018.06.037.

[16] H.-C. Chiu *et al.*, "High-performance normally off p-GaN Gate HEMT with composite $AlN/Al_{0.17}Ga_{0.83}N/Al_{0.3}Ga_{0.7}N$ barrier layers design," *IEEE Electron Devices Soc.*, vol. 6, no. 1, pp. 201–206, Jan. 2018, doi: 10.1109/JEDS.2018.2789908.

[17] R. Hao *et al.*, "Studies on fabrication and reliability of GaN high-resistivity-cap-layer HEMT," *IEEE Trans. Electron Devices*, vol. 65, no. 4, pp. 1314–1320, Apr. 2018, doi: 10.1109/TED.2018.2803521.

[18] C. Sun *et al.*, "Normally-off p-GaN/AlGaN/GaN high-electron-mobility transistors using oxygen plasma treatment," *Appl. Phys. Exp.*, vol. 12, no. 5, Apr. 2019, Art. no. 051001, doi: 10.7567/1882-0786/ab0b78.

[19] S. J. Pearton, H. Cho, J. R. LaRoche, F. Ren, R. G. Wilson, and J. W. Lee, "Oxygen diffusion into SiO_2-capped GaN during annealing," *Appl. Phys. Lett.*, vol. 75, p. 2939, Nov. 1999, doi: 10.1063/1.125194.

[20] H.-C. Chiu *et al.*, "High uniformity normally-off p-GaN gate HEMT using self-terminated digital etching technique" *IEEE Trans. Electron Devices*, vol. 65, no. 11, pp. 4820–4825, Nov. 2018, doi: 10.1109/TED.2018.2871689.

[21] R. Hao *et al.*, "Breakdown enhancement and current collapse suppression by high-resistivity GaN cap layer in normally-off AlGaN/GaN HEMTs," *IEEE Electron Device Lett.*, vol. 38, no. 11, pp. 1567–1570, Nov. 2017, doi: 10.1109/LED.2017.2749678.

[22] H. Ishida *et al.*, "Unlimited high breakdown voltage by natural super junction of polarized semiconductor," *IEEE Electron Device Lett.*, vol. 29, no. 10, pp. 1087–1089, Oct. 2008, doi: 10.1109/LED.2008.2002753.

XINKE LIU (Member, IEEE) received the B.Appl.Sc. degree (Hons.) in materials science in 2008 and the Ph.D. degree in electrical and computer engineering from the National University of Singapore in 2013. He is currently an Assistant Professor/Research Professor with Shenzhen University, China. He has authored or coauthored more than 100 journal and conference papers, and his research is related to GaN-based power devices.

HSIEN-CHIN CHIU (Senior Member, IEEE) received the Ph.D. degree in electrical engineering from National Central University, Zhongli, Taiwan, in 2003. He is currently a Professor with the Department of Electronic Engineering, Chang Gung University (CGU), Taoyuan, Taiwan, where he also served as the Director of High Speed Intelligent Communication Research Center from 2012. He was invited to join the publicity and marketing team of Adcom Committees Organization in IEEE Microwave Theory and Techniques Society. He has authored or coauthored more than 180 SCI journal publications. His research interests include the microwave, millimeter wave integrated circuits, GaAs and GaN FETs fabrication, and modeling. He is a member of Phi Tau Phi.

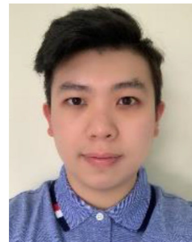

CHIA-HAO LIU received the M.S. degree from the Department of Electron Engineering, Chang Gung University, Taoyuan, Taiwan, in 2019, where he is currently pursuing the Ph.D. degree. He is interest in III-V compound semiconductor power devices.

HSUAN-LING KAO received the B.S. degree in electrical engineering from Chang Gung University, Taoyunan, in 1998, and the M.S. and Ph.D. degrees in electronics engineering from National Chiao Tung University, Hsinchu, Taiwan, in 2000 and 2006, respectively. From 2000 to 2006, she was with Macronix Company, Hsinchu, Taiwan. Since October 2006, she has been with Department of Electronics Engineering, Chang Gung University, Taoyunan, Taiwan, and is currently a Professor. She is a Technical Reviewer for the IEEE TRANSACTIONS ON INDUSTRIAL ELECTRONICS, the IEEE ELECTRON DEVICE LETTERS, the IEEE TRANSACTIONS ON MICROWAVE THEORY AND TECHNIQUES, and *International Journal of Electronics*. Her current research interests include microwave and millimeter-wave devices and integrated circuits.

CHAO-WEI CHIU received the M.S. degree in electrical engineering from National Taiwan Ocean University, Keelung, Taiwan, in 2009. He is a Research Assistant with the Department of Electrical Engineering, Chang Gung University, Taoyuan, Taiwan. He is interested in III-V compound semiconductor power and microwave devices fabrications.

HSIANG-CHUN WANG received the Ph.D. degree from Chang Gung University, Taoyuan, Taiwan, in 2014. His research interests GaN-based power devices and materials.

JIANWEI BEN received the Ph.D. degree in condensed matter physics from the Changchun Institute of Optics, Fine Mechanics and Physics, Chinese Academy of Sciences in 2019. He is currently a Postdoctoral Researcher with Shenzhen University, China. He has authored or coauthored more than 8 journal papers. His research is related to the growth of III-nitride semiconductor materials.

WEI HE received the bachelor's degree in communication engineering from Xiamen University in 2003, and the Ph.D degree in microelectronics and solid electronics from the Shanghai Institute of Micro Systems and Information Technology, Chinese Academy of Sciences in 2008. He is currently an Associate Professor/Research Professor with Shenzhen University, China. He has authored or coauthored more than 30 journal and conference papers. His main research fields include new semiconductor device structure and large-scale integrated circuit design.

CHONG-RONG HUANG received the M.S. degree from the Department of Electron Engineering, Chang Gung University, Taoyuan, Taiwan, in 2019, where he is currently pursuing the Ph.D. degree. He is interest in III-V compound semiconductor microwave and power electronics applications.